WAVE PROPAGATION IN THE SUN AND THE INTERPRETATION OF HELIOSEISMIC DATA

A DISSERTATION
SUBMITTED TO THE DEPARTMENT OF PHYSICS
AND THE COMMITTEE ON GRADUATE STUDIES
OF STANFORD UNIVERSITY
IN PARTIAL FULFILLMENT OF THE REQUIREMENTS
FOR THE DEGREE OF
DOCTOR OF PHILOSOPHY

Aaron C Birch
May 2002

I certify that I have read this dissertation and that in my opinion it is fully adequate, in scope and quality, as a dissertation for the degree of Doctor of Philosophy.

Philip Scherrer
(Principal Adviser)

I certify that I have read this dissertation and that in my opinion it is fully adequate, in scope and quality, as a dissertation for the degree of Doctor of Philosophy.

Alexander Kosovichev

I certify that I have read this dissertation and that in my opinion it is fully adequate, in scope and quality, as a dissertation for the degree of Doctor of Philosophy.

Robert Wagoner

Approved for the University Committee on Graduate Studies:

Abstract

In order to better understand the physics of the Sun it is necessary to obtain observational constraints on the temporal variations of the flows and structures in the interior of the Sun. Helioseismology, the use of waves to probe the solar interior, has been developed over the course of several decades and has led to numerous exciting results regarding the solar interior. This dissertation is mainly an effort to develop the theory necessary for the interpretation of time-distance helioseismology data.

The results contained in this dissertation can be placed in three broad categories: oscillations in magnetized atmospheres, models for the interpretation of time-distance helioseismology data, and observational results derived using global mode and time-distance helioseismology. We show that in both isothermal and polytrope atmospheres with weak vertical magnetic fields acoustic modes exist, as do numerous magnetic modes. The magnetic modes can become unstable in the vicinity of avoided crossings.

Time-distance helioseismology, which measures the travel times for wave packets moving between distinct points on the solar surface, has provided many intriguing results. It is not yet well understood how to interpret the data, i.e. how to relate subsurface perturbations to the observed travel times. We demonstrate that the Born approximation agrees well with direct numerical results for weak sound-speed perturbations. We also develop a general recipe for the calculation of the sensitivity of travel times to subsurface perturbations, using a physically motived distributed wave-source model.

One of the two main observational studies in this dissertation is of near-pole solar rotation. We perform Optimally Localized Averaging (OLA) inversions of MDI and GONG normal-mode frequency splittings to estimate the average, over the upper 4% of the convection zone, of the north-south symmetric component of rotation.

Closer than 20° to the poles we obtain a rotation rate that is 10 nHz slower than would be expected from a smooth extrapolation from lower latitudes. A preliminary analysis of frequency splittings from the Big Bear Solar Observatory suggests that the near-pole rotation rate is time dependent.

The second observational study is a search for longitudinal variation in the sound speed in the convection zone. We show synoptic charts, for three Carrington rotations, of sound speed as a function of depth inferred by the inversion of deep-focusing time-distance data. These charts show what may be structures in the deep convection zone or may be the effect of near-surface magnetic field. We are able to place a rough upper limit of 10^6 gauss on the variations in the magnetic field in the tachocline. These measurements of the near-pole rotation rate and the longitudinal structure of the sound-speed profile are important for understanding variations of the internal structure and rotation with the solar cycle and the mechanisms of the solar dynamo.

Acknowledgements

First of all I would like to thank Phil Scherrer and Sasha Kosovichev for their help and guidance over the years. Laurent Gizon has played a central role in my education over the past five years; I am grateful to have had the opportunity to discuss so many interesting research problems with him. Tom Duvall and Jesper Schou have also been important in my efforts to learn something about helioseismology. I also would like to thank my collaborators for teaching me so much. The SOI research group has been an amazing place to work; I thank everyone here for making research such an interesting activity. I am grateful for the time that Brian Roberts and Keh-Cheng Chu have put into making sure that my computer keeps running. I thank Margie Stehle for the help she has given me.

I thank Anita and Steve for their hospitality over the years. And a thanks to Dave and Lexa for the good times. Thanks to Gary and Ross for the conversations and experiences that we have shared. I also would like to thank the tube-or-not-tubers and bumpies, in particular Mike, John, David, Craig, and Cathryn. Thanks to Tricia and Molly for their friendship over all this time. Thanks to the Stanford crew (Tim, Emily, Veronica, Phil, John, Danna, Aaron, Holly, Nicci, Fil, Travis, Taska, Tarek, and Dave) for making the past six years so interesting and entertaining.

Finally, thanks to my parents, my grandparents, my brother, and Kelsey for their support.

Contents

Abstract **v**

Acknowledgements **vii**

1 Introduction **1**

1.1 Motivation 1

1.2 Results Contained in This Work 2

1.3 A Brief Review of Helioseismology 3

1.4 The Governing Equations 6

1.5 Observations of Solar Oscillations: MDI, GONG, and BBSO 11

1.5.1 Dopplergrams 12

1.5.2 Power Spectra, Frequencies, Cross-correlations, and Travel Times 13

1.5.3 Inversions of the Data 15

2 Oscillations in Magnetized Atmospheres **16**

2.1 Introduction 17

2.2 The Resonant Hopf Bifurcation 18

2.3 Equations and Equilibria 19

2.4 Linear Theory 21

2.5 Numerical Results 23

2.6 Large Cooling Time 23

2.7 Small Cooling Time 28

2.8 A Resonant Hopf Bifurcation 28

2.9 Islands of Reality: the Onset of Complex Eigenvalues 31

2.10 Discussion 33

3 Theoretical Interpretation of Time-Distance **35**

3.1 Introduction 35

3.2 Single-Source Model for Travel-Time Sensitivities 38

3.2.1 Derivation of Travel-Time Sensitivities 39

3.2.2 The Born Approximation and Normal Mode Coupling 45

3.2.3 Numerical Examples 47

3.3 The Accuracy of the Born and Ray Approximations 51

3.3.1 Methods 54

3.3.2 Results 55

3.4 A Distributed Source Model for Travel Times 60

3.4.1 A General Theory 60

3.4.2 A Surface Gravity Wave Example 73

4 Results of Analysis of Helioseismic Data **98**

4.1 An Introduction to Inversions 98

4.2 Subsurface Rotation from MDI, GONG, and BBSO 100

4.2.1 The Data 100

4.2.2 Inversion Method 101

4.2.3 Averaging Kernels 103

4.2.4 Testing on Artificial Data 104

4.2.5 Results from MDI, GONG, and BBSO 107

4.3 A Time-Distance Search for Longitudinal Structure 114

4.3.1 The Data and Deep Focusing 115

4.3.2 Measurement of Travel Times 116

4.3.3 Travel-Time Kernels 119

4.3.4 OLA Inversion 122

4.3.5 Effect of Surface Magnetic Field 125

4.3.6 Interpretation in Terms of Deep Magnetic Field 128

5 Discussion **131**

5.1 Future Work 137

A Adiabatic Magneto-Acoustic Oscillations **138**

B Definition of Travel Time **141**

C Fourier Conventions **143**

D Two-Dimensional Travel-Time Kernels **145**

E Two-Dimensional Single-Source Kernels **148**

F Derivation of Deep-Focusing Kernels **150**

F.1 Green's Function 152

F.2 Zero-Order Cross-Correlation 153

F.3 Power Spectrum 154

F.4 Derivation of Kernels 155

G Time-Domain Calculation of 3D Kernels **158**

H Descriptions of Some Useful Codes **160**

H.1 Normal Mode Calculations 160

H.2 Ray Calculations 161

Bibliography **170**

List of Figures

1.1 Observed and model surface gravity wave cross-correlations 14

2.1 Solutions to a complex quadratic 20
2.2 Dispersion relation for an $m = 2$ polytrope with weak magnetic field. 24
2.3 Comparison of frequencies in the isothermal and polytrope atmospheres with weak magnetic field 25
2.4 Dispersion relation for a polytrope with strong damping 27
2.5 Comparison of frequencies in polytrope and isothermal layers with strong damping 29
2.6 Frequencies as function of damping rate for a polytrope 30

3.1 Slices through a travel-time kernel 48
3.2 Comparison of Born and ray kernels 50
3.3 Born and ray approximation travel times 51
3.4 A frame from a finite difference calculation of the pressure field . . . 53
3.5 Cross-correlations between the waveform at the receiver and the unperturbed waveform 56
3.6 Travel-times shifts for uniform spheres 58
3.7 Travel times for smooth spheres as functions of sphere HWHM 59
3.8 Measuring travel times from cross-correlations 62
3.9 Two types of contributions to the first-order perturbation to the cross-correlation 70
3.10 The basic setup for the example 74
3.11 The wavenumber dependence of the filter F and of the OTF 82
3.12 A comparison of observed and model power spectra 86

3.13 Travel-time sensitivity kernels for perturbations in source strength and damping rate 90
3.14 Cuts through the source and damping kernels 93
3.15 Comparison between single- and distributed-source kernels 95
3.16 Cuts along the line $y = 0$ through the damping kernels 96
3.17 A graphical discussion of the single-source picture 97

4.1 Latitudinally integrated averaging kernels 105
4.2 Latitudinal dependence of averaging kernels 106
4.3 Inversion result for artificial data 108
4.4 OLA inversions of GONG and MDI frequency splitting data 109
4.5 OLA inversions of GONG and MDI data with smooth fit removed . . 110
4.6 Rotation inversions with a smooth fit removed 111
4.7 OLA inversion of BBSO data 112
4.8 Deviations of inversions of BBSO data from the mean rotation 113
4.9 Ray paths for deep-focusing 117
4.10 Deep-focusing travel times 118
4.11 Deep-focus travel times for the shallowest and deepest foci 120
4.12 Error estimates for deep-focusing travel times 121
4.13 Deep-focusing travel-time kernels for sound speed 123
4.14 Choosing the trade-off parameter 124
4.15 Inferred sound speed perturbation 126
4.16 Spatial weights for averaging surface magnetic field 127
4.17 Effect of surface magnetic field on the inversion 129

Chapter 1

Introduction

1.1 Motivation

There are a number of important unsolved problems in solar physics: for example, the dynamo process, the dynamics of differential rotation, and the existence of active longitudes. By the dynamo process I mean the process by which the large scale magnetic field of the Sun is generated over the course of the solar cycle. The differential rotation profile of the Sun is also observed to change throughout the solar cycle. There have been many claims that there are "active longitudes", preferred longitudes for activity (e.g. flares, coronal mass ejections, active regions). These active longitudes may be tied to the dynamo process, for example by longitudinal variation in the magnetic field in the tachocline (the region of sharp radial gradient in the rotation rate located at the base of the convection zone).

Understanding of the dynamo process, the nature of active longitudes, and the physical mechanisms responsible for differential rotation will come as a result of theory and modeling. Theory and modeling are, however, driven by improved measurements, for example of subsurface flows, magnetic field, and local temperature inhomogeneities. Helioseismology is the only tool that will be used to make these measurements. As a result, the development of the techniques of helioseismology and the application of these techniques to measure basic solar properties is important for the progress of solar physics.

In particular, the emerging field of time-distance helioseismology has delivered

many exciting results. The theoretical basis for the interpretation of time-distance data lags far behind the observational work that is currently being done. Time-distance helioseismology is particularly important because of the upcoming SDO mission (http://lws.gsfc.nasa.gov/sdo.htm), which will provide high-resolution full-disk data. A substantial amount of the work in this dissertation is an attempt to build a solid theoretical foundation for the interpretation of time-distance data.

1.2 Results Contained in This Work

The results contained in this dissertation fall in three main categories: some aspects of oscillations in magnetized atmospheres, conclusions concerning the forward problem for time-distance helioseismology (this is the most substantial chapter in this work), and observational results derived using global mode and time-distance helioseismology. The remainder of Chapter 1 gives a brief review of the field of helioseismology, with an emphasis on local helioseismology. I will also give a quick introduction to the observational procedures, as well as a description of the basic governing equations for linear oscillations.

Chapter 2 is a study of the linear stability of oscillations in a weakly magnetized atmosphere, in the MHD approximation. This problem is important for understanding the effects of magnetic field on oscillations, and the role of magnetic field in dynamical processes in the solar atmosphere. Non-adiabatic effects are modeled using Newton's law of cooling. The main result of the chapter is that in general the $k-\omega$ diagram is quite complicated, with avoided crossings and mergers between different branches of the dispersion relation. In the vicinity of avoided crossings overstable modes can exist. This model was originally developed as an attempt to explain solar spicules (highly localized chromospheric events associated with magnetic field) as a result of the nonlinear development of overstable oscillations, by analogy with oscillons (localized temporally oscillating solutions to nonlinear partial differential equations, e.g. Umurhan et al., 1999). In this model the acoustic modes, other than the Lamb mode, appear to be only slightly modified by the magnetic field.

Chapter 3 is about the forward problem for time-distance helioseismology, i.e. the dependence of travel times on subsurface perturbations. This provides a basis

for the interpretation of experimental data. We show that, in the Born approximation, travel times are insensitive to sound-speed perturbations located on the ray connecting the two observation points, in contrast with ray theory which says that the sensitivity should only be non-zero along the ray path. The second section of chapter 3 is a numerical study of the accuracy of the Born and ray approximations for calculating travel-time perturbations. We show that the Born approximation essentially always provides superior accuracy than the ray approximation, and verify by comparison with numerical solutions of the wave equation the prediction of zero sensitivity along the ray path. Finally, chapter 3 gives a general approach for the calculation of Born approximation travel-time sensitivities in random distributed wave-source models and shows, for a simple surface gravity wave example, that the single-source approximation is not qualitatively correct.

Chapter 4 contains two studies involving observational data. The first is an inversion of MDI, GONG, and BBSO frequency splittings. We use Optimally Localized Averaging (OLA) inversion to estimate the symmetric component of the solar rotation rate averaged in depth over the upper 4% of the convection zone. Closer than 20° to the poles the inferred rotation rate is approximately 10 nHz slower than would be expected from a smooth extrapolation from lower latitudes. A preliminary analysis of frequency splittings from the Big Bear Solar Observatory suggests that the near-pole rotation rate is time dependent. In addition zonal flows are seen with both MDI and GONG p-mode frequency splittings.

The second study is of the longitudinal dependence of the sound speed in the convection zone using time-distance helioseismology with MDI data. We show synoptic sound-speed maps, that show hints of resolved structures in the lower convection zone, for three rotations in the year 2000. This study is the first attempt at obtaining a longitudinally resolved view of solar activity in the deep convection zone.

1.3 A Brief Review of Helioseismology

Solar oscillations, with periods around five minutes, were first observed by Leighton et al. (1962). These oscillations were later identified as standing acoustic waves in the solar interior by Ulrich (1970) and Leibacher & Stein (1971). Soon after,

measurements of the frequencies of these normal modes were used to constrain the interior rotation rate and sound speed in the Sun. The term "helioseismology", meaning the use of solar oscillations as probes of internal solar structure, entered general use in the literature in 1983.

Normal mode based helioseismology has traditionally been described in two parts: the forward problem and the inverse problem (e.g. Gough, 1985). The forward problem for normal mode helioseismology is to predict the dependence of normal mode frequencies on subsurface conditions. The analytical and numerical techniques for solving the normal-mode forward problem are well developed (e.g. Christensen-Dalsgaard, 1994). Furthermore, current solar models give normal mode frequencies that reproduce the observed frequencies to roughly 0.1% (e.g. Li et al., 2002). The inverse problem, using observed frequencies to constrain subsurface rotation and structure, has also been substantially developed over the past twenty years.

The two main goals of normal mode helioseismology have been to determine the rotation rate as a function of depth and latitude and the spherical average of the sound speed as a function of depth. Currently, inferences of the internal sound speed agree with solar models to better than 0.25% (e.g. Basu et al., 1997). Attempts, using simulations of solar convection, are under way (e.g. Miesch et al., 2000) to model the observed rotation rate (e.g. Schou et al., 1998) as well. The new targets of normal mode helioseismology studies are effects that are time-varying and on spatial scales that are much smaller than global, for example torsional oscillations (e.g. Howe et al., 2000a), the temporal variation of rotation in the tachocline (Howe et al., 2000b), and time variations of the shape of the tachocline (e.g. Basu & Antia, 2001).

Standard normal mode helioseismology is limited to studying azimuthally and north-south averaged quantities. There are numerous features on the Sun which are fundamentally three-dimensional, for example sunspots, active regions, and supergranulation. Furthermore, large scale flows are not necessarily north-south symmetric, for example the torsional oscillations. Meridional flow (flow along meridians), even the north-south symmetric component, does not effect normal mode frequencies to lowest order and therefore cannot be studied by standard normal mode helioseismology. As a result, local methods are necessary to study the many features on the

Sun which are not easily probed with a normal mode based approach.

Three main forms of local helioseismology are currently in common use. Ring-diagrams (Hill, 1988) fit three-dimensional power spectra measured over local patches on the solar surface. Time-distance helioseismology (Duvall et al., 1993b) measures travel times for wave packets moving between pairs of points on the surface. Acoustic holography (Lindsey & Braun, 1997) is based on the use of back-projection of the observed wavefield to identify inhomogeneities in the interior.

The interpretation of ring-diagram measurements has been strongly based on the traditional normal-mode approach. The observed power spectra are fitted, and the fitting parameters are related to solar subsurface conditions using a normal-mode based interpretation. In particular, the issue of the horizontal sensitivity of fit parameters to subsurface conditions has been largely neglected. The two main results of ring-diagram analysis are measurements of large-scale flows in the upper convection zone (e.g. Haber et al., 2000; Hernandez et al., 2000) and the dependence of local frequencies on the presence of active regions (e.g. Rajaguru et al., 2001).

There has been some preliminary work on modeling the sensitivity of holographic measurements to the local strength of acoustic sources (Skartlien, 2001). The sensitivity of phase-sensitive holography to local flows and sound speed perturbations is not yet well understood. Holography shows a clear signal around active regions (e.g. Braun & Lindsey, 2000) though the cause of this signal is not known. A stunning result obtained with phase-sensitive holography was the demonstration that magnetic field on the back side of the Sun could be detected (Lindsey & Braun, 2000), though again the meaning of the signal is not clear.

Time-distance helioseismology, which is a focus of this dissertation, has been used in studies of sunspots (e.g. Duvall et al., 1996; Kosovichev et al., 2000; Zhao et al., 2001), supergranulation (Duvall & Gizon, 2000), and meridional flow (e.g. Giles et al., 1997). The interpretation of time-distance data has been done mainly in the ray approximation (e.g. D'Silva et al., 1996; Kosovichev, 1996a; Zhao et al., 2001). Relatively early on it was pointed out that ray theory is not entirely appropriate as time-distance analysis employs waves with substantial wavelengths (Bogdan & Cally, 1997). Birch & Kosovichev (2000) and Jensen et al. (2000) solved the linear finite-wavelength forward problem for sound-speed perturbations, in the

single-source approximation. The distributed source problem was solved, in the Born approximation, by Gizon & Birch (2002).

All of the techniques of helioseismology are based on an understanding of wave propagation in the Sun, which is necessary to model the sensitivity of observables (frequencies, travel times, etc.) to subsurface perturbations.

1.4 The Governing Equations

In this section I will write down and discuss the equations of motion for solar plasma in the magnetohydrodynamics (MHD) approximation. The MHD equations are standard; detailed discussions and derivations can be found in standard textbooks (e.g. Jackson, 1975).

The first approximation that is necessary to obtain the MHD equations is that the gas be treated as a continuum rather than as a collection of individual particles. This approximation implies that there is a length scale that is much smaller than the length scales of interest in the problem but still much larger than the inter-particle spacing. In the photosphere the number density of particles is of order 10^{23} m^{-3}, as a result the average distance between particles is of order 10^{-8} m. The length scales that are currently of interest to helioseismology are at smallest 10^{5} m, a fraction of a granule. These two scales are vastly disparate, as a result the continuum approximation is good.

A direct result of the continuum approximation is the continuity equation:

$$\dot{\rho} + \boldsymbol{\nabla} \cdot (\rho \boldsymbol{v}) = 0 \,. \tag{1.1}$$

The mass density of the plasma is given by ρ and the velocity by $\boldsymbol{v}$. The overdot denotes the partial derivative with respect to time, a notation that will be used throughout this dissertation. The mass density is the mass per unit volume, a concept that is only well defined on length scales much larger than the inter-particle spacing.

With the assumption that the plasma is everywhere electrically neutral the momentum equation can be written as

$$\rho\frac{D\boldsymbol{v}}{Dt} = -\boldsymbol{\nabla}p + \frac{1}{c_\mathrm{l}}\mathbf{J}\times\mathbf{B} + \rho\mathbf{g}\,. \tag{1.2}$$

The speed of light is c_l, the subscript l is present to avoid confusion with the sound speed c which will appear many times in this dissertation. The viscous terms in the momentum equation have been neglected as the viscous time scale $T_\nu = L^2/\nu$ (L is the length scale of the waves and ν the kinematic viscosity) is large compared to five minutes, the period of the waves that we are interested in. Duvall & Gizon (2000) obtained an estimate of $\nu = 250$ km^2 s^{-1} in the photosphere, which for a length scale of $L = 5$ Mm gives $T_\nu \approx 28$ hours. The pressure p is assumed to be scalar. The term $\rho\mathbf{g}$ is due to the force of gravity on the fluid, where $\mathbf{g}$ is the local value of the gravitational acceleration. The term $\rho_e\mathbf{E}$ due to the electric field, $\mathbf{E}$, acting on the local charge density, ρ_e, has been neglected as a result of the assumption that the plasma is electrically neutral. The Lorentz force appears as $\frac{1}{c_\mathrm{l}}\mathbf{J}\times\mathbf{B}$. The electric current is $\mathbf{J}$ and the magnetic field is $\mathbf{B}$, related by $\mathbf{J} = \frac{c_\mathrm{l}}{4\pi}\boldsymbol{\nabla}\times\mathbf{B}$. Notice that the displacement current $\dot{\mathbf{E}}$ has been neglected as we are working in the MHD approximation. The operator D/Dt is the standard material derivative

$$\frac{D\phi}{Dt} = \frac{\partial\phi}{\partial t} + (\boldsymbol{v}\cdot\nabla)\,\phi\,. \tag{1.3}$$

Gravitational acceleration can be computed from the distribution of density, via the gravitational potential Φ,

$$\Phi(\boldsymbol{x}) = -G\int \mathrm{d}\boldsymbol{r}\,\frac{\rho(\boldsymbol{r})}{|\boldsymbol{x}-\boldsymbol{r}x|}\,. \tag{1.4}$$

The integral $\int \mathrm{d}\boldsymbol{r}$ denotes integration over all space. The local gravitational acceleration can be obtained from the gravitational potential,

$$\mathbf{g} = -\boldsymbol{\nabla}\Phi\,. \tag{1.5}$$

In the ideal MHD limit the conductivity σ is infinite. This approximation is

reasonable for five minute waves in the Sun where resistive time scales are very large, of order a year for thin flux tubes and of order 10^{10} years for global scale features (Schrijver & Zwaan, 2000). In the ideal MHD approximation the current $\mathbf{J}$ in the frame moving with the fluid is zero. As a consequence, in the moving frame the electric field is balanced by the Lorentz force,

$$\mathbf{E} + \frac{1}{c_{\rm l}} \boldsymbol{v} \times \mathbf{B} = 0 \,. \tag{1.6}$$

This equation can be used to write the MHD equations without reference to the electric field. In particular Faraday's law can be written as

$$\dot{\mathbf{B}} = \boldsymbol{\nabla} \times (\boldsymbol{v} \times \mathbf{B}) \,. \tag{1.7}$$

There are a number of forms that the energy equation could be written in. In the case where the heat capacity at constant volume, C_v, is constant the energy per unit mass of the plasma can be written as

$$\epsilon = \frac{1}{2} \boldsymbol{v}^2 + C_v T \tag{1.8}$$

and the energy equation reduces to

$$\rho C_v \frac{DT}{Dt} + p \nabla \cdot \boldsymbol{v} = Q(T, \rho) \tag{1.9}$$

(e.g. Chandrasekhar, 1981). The temperature is denoted by T and $Q(T, \rho)$ is a function which describes the heat lost by radiation as a function of temperature and density. Additional terms could be included in this equation to include other forms of heat loss, for example by thermal conductivity (e.g. Chandrasekhar, 1981).

The equation of state gives the pressure as a function of density and temperature. The simplest equation of state is that of an ideal gas

$$p = \frac{R \rho T}{\mu} \,. \tag{1.10}$$

The mean molecular weight is μ and the gas constant is R. In general, the equation of state for solar plasma is quite complicated as it must account for the temperature

dependence of ionization and the variation of the chemical composition with radius in the Sun. In chapter 2 we use the ideal gas equation of state with constant mean molecular weight. Elsewhere we use the adiabatic approximation (eq. [1.18]), which makes a specification of the equation of state unnecessary (once the sound speed is known) for calculations of small amplitude waves.

Linearization of the Equations of Motion

The full nonlinear set of MHD equations is in general quite difficult to treat mathematically and as a result some simplifications are convenient. The approximation of linear waves moving through a stationary background will be used throughout this dissertation. In particular, each of the properties of the plasma will be written as a background value plus a first order wave quantity, e.g.

$$\rho = \rho_0 + \rho' \,. \tag{1.11}$$

In this section, the subscript 0 will be used to denote background quantities and the superscript $'$ to denote wave variables. To further simplify the resulting equations, I will consider only background states that are static, i.e. $\boldsymbol{v}_0 = \mathbf{0}$.

From the equations obtained earlier in this section and expansions of the form of equation (1.11), I obtain the equations for the steady background state

$$\boldsymbol{\nabla} p_0 = \rho_0 \mathbf{g} + \frac{1}{c_{\rm l}} \mathbf{J}_0 \times \mathbf{B}_0 \,, \tag{1.12}$$

$$\mathbf{J}_0 = \frac{c_{\rm l}}{4\pi} \boldsymbol{\nabla} \times \mathbf{B}_0 \,. \tag{1.13}$$

Equation (1.12) is the statement that in the background state the pressure gradient balances the force of gravity and the Lorentz force. Notice that the continuity equation is automatically satisfied in the background state where the plasma velocity is zero and time derivatives are zero.

Linearizing in the wave variables $\rho', p', \boldsymbol{v}'$, and $\mathbf{B}'$ gives the equations of motion:

$$\dot{\rho}' + \rho_0 \boldsymbol{\nabla} \cdot \boldsymbol{v}' = 0\,, \tag{1.14}$$

$$\rho_0 \dot{\boldsymbol{v}}' - \boldsymbol{\nabla} p' = \frac{1}{4\pi}\{(\boldsymbol{\nabla} \times \mathbf{B}_0) \times \mathbf{B}' + (\boldsymbol{\nabla} \times \mathbf{B}') \times \mathbf{B}_0\} + \rho' \mathbf{g}\,, \tag{1.15}$$

$$\rho_0 C_v \dot{T}' + p_0 \boldsymbol{\nabla} \cdot \boldsymbol{v}' = \frac{\partial Q}{\partial T}(T_0, \rho_0) T' + \frac{\partial Q}{\partial \rho}(T_0, \rho_0)\rho'\,, \tag{1.16}$$

$$\dot{\mathbf{B}}' = \boldsymbol{\nabla} \times (\boldsymbol{v}' \times \mathbf{B}_0)\ . \tag{1.17}$$

Equation (1.14) is the linearized continuity equation. Conservation of momentum is described by equation (1.15). The three forces on the fluid are the pressure gradient, gravity, and the Lorentz force which in this case is expressed entirely in terms of the magnetic field. Equation (1.16) is the linearized heat equation; notice that the heat loss function Q has been linearized in temperature and density around the background values. Finally, equation (1.17) gives the time evolution of the magnetic field perturbation in terms of the plasma velocity and the background magnetic field.

Notice in equation (1.15) that I have employed the Cowling approximation, i.e. neglected the effect of waves on the gravitational acceleration. The Cowling approximation will be used throughout this dissertation, except in the numerical computation of zero-order frequencies and eigenfunctions for solar oscillations. Christensen-Dalsgaard & Berthomieu (1991) discuss the validity of the Cowling approach for solar oscillations; they show by direct numerical calculations that the error introduced by the Cowling approximation is less than 1% at $l = 20$ and decreases with increasing l, where l is angular degree.

In helioseismology the adiabatic approximation, $Q = 0$, is commonly employed. The justification is that observed mode damping rates are of order μHz (e.g. Komm et al., 2000), three orders of magnitude smaller than mode frequencies. In this approximation the Lagrangian pressure and density perturbations, δp and $\delta\rho$ respectively, are related by

$$\delta p = c^2 \delta\rho \tag{1.18}$$

where c^2 is the square of the local sound speed (e.g. Christensen-Dalsgaard, 1994). For adiabatic waves the above equation can be used in place of equation (1.16). In this dissertation the adiabatic approximation is employed everywhere except in

chapter 2, which is primarily an investigation of the effect of non-adiabaticity.

Wave Propagation in the Sun

The equations in the previous section tell us how to compute the wavefield once we know the source of waves and the background state. In the Sun waves are mainly excited by near surface turbulence (e.g. Stein, 1967). This process is in general quite complicated to model, in this dissertation only simple phenomenological models are employed (e.g. section 3.4). The background state for the Sun is quite well known, as a result of global mode helioseismology, except in the very near surface layers and the deep core.

The two types of waves that are currently important to helioseismology are the f modes and p modes. The f mode is a surface gravity wave, the restoring force is gravity. The p mode is the acoustic wave, the restoring force is pressure. Also expected to be observed, eventually, is the g mode, the internal gravity wave, where buoyancy is the restoring force. Christensen-Dalsgaard (1994) gives simple models for each of these three types of waves and derives approximate dispersion relations. In the presence of magnetic field the situation is substantially more complicated (see e.g. Jackson, 1975, for a brief discussion of MHD waves). The second chapter of this dissertation investigates the modes of simple magnetized isothermal and polytrope slabs.

1.5 Observations of Solar Oscillations: MDI, GONG, and BBSO

This dissertation uses helioseismology data from three different sources: MDI, GONG, and BBSO. MDI (Michelson Doppler Imager) is an instrument on the SOHO (SOlar and Heliospheric Observatory) spacecraft (Scherrer et al., 1995). GONG (Global Oscillations Network Group) is a world-wide collection of telescopes with continuous coverage of the Sun (Harvey et al., 1988). BBSO (Big Bear Solar Observatory) is a solar observatory at Big Bear Lake in California. The BBSO data I have used are described by Woodard & Libbrecht (1993). Each of these experiments measures

images of the line-of-sight component of the Doppler velocity, computed from the Doppler shift of an absorption line, over the Solar disk.

1.5.1 Dopplergrams

The fundamental data of modern helioseismology are high-resolution Doppler images of the Sun's surface. In general, the filtered line-of-sight projection of the velocity field can be written as

$$\phi = \mathcal{F}\left\{\hat{\boldsymbol{\ell}} \cdot \boldsymbol{v}\right\} . \tag{1.19}$$

The operator $\mathcal{F}$ describes the filter used in the data analysis, which includes the time window and instrumental effects (as well as any filters imposed during the data analysis). The unit vector in the direction of the line of sight is $\hat{\boldsymbol{\ell}}$. The velocity of the plasma where the line is formed is $\boldsymbol{v}$. For example, MDI measures the line-of-sight Doppler velocity using a line formed at a height of 300 km above the photosphere. Acoustic modes, except those with frequencies above the acoustic-cutoff, are reflected downwards (due to an increase with height of the acoustic-cutoff frequency) before they reach the photosphere. The observations are therefore not of vertically propagating waves, but rather of their evanescent tails. The f mode is quite different as it propagates only in the horizontal direction and has an energy density that is concentrated near the photosphere (e.g. Duvall & Gizon, 2000).

The cadence for the MDI, GONG, and BBSO data used in this dissertation is one Doppler map (Dopplergram) per minute. This cadence is reasonable as it gives a Nyquist frequency of 8.3 mHz, well above the frequencies of the bulk of the p modes. For MDI in its high-resolution mode the spatial resolution is $1.2''$ (0.8 Mm on the Sun at disk center). In full-disk mode the resolution of MDI is $4''$. BBSO Dopplergrams have 192×240 pixels and cover the full disk (Woodard & Libbrecht, 1993), giving a spatial resolution of approximately 7×6 Mm at disk center. The GONG Dopplergrams have 256×242 pixels and also cover the full-disk (e.g. Leibacher & the GONG Project Team, 1998), which gives a resolution of roughly 5.5 Mm at disk center.

1.5.2 Power Spectra, Frequencies, Cross-Correlations, and Travel Times

Power Spectra

Normal-mode helioseismology uses the spherical harmonic and temporal Fourier transforms of Dopplergrams. Spherical harmonics are labeled by angular degree $l \geq 0$ and azimuthal order m with $|m| \leq l$. The result of the spherical harmonic transform and temporal Fourier transform of a series of Dopplergrams is thus a function of temporal frequency, angular degree l, and azimuthal order m. The square of the absolute value of the transform is the power spectrum.

Normal Mode Frequencies

Normal mode frequencies are obtained by fitting the resonance peaks in the spectra (e.g. Schou, 1992). There are a number of subtleties involved in measuring frequencies, for example the frequency depends on the model which is used to obtain the shape of the peaks in the spectrum. A further complication is that the spherical harmonics are not orthogonal over the visible disk. As a result the spherical harmonic transforms of the data do not perfectly separate the signal from different modes. At high l, the leaks are a serious problem, the individual l's cannot be distinguished in the spectrum and complicated ridge-fitting techniques are necessary.

Cross-Correlation

The basic computation in time-distance helioseismology is the temporal cross-correlation, $C(\mathbf{1}, \mathbf{2}, t)$, between the signal, ϕ, measured at two points, $\mathbf{1}$ and $\mathbf{2}$, on the solar surface,

$$C(\mathbf{1}, \mathbf{2}, t) = \frac{1}{T} \int_0^T \mathrm{d}t' \; \phi(\mathbf{1}, t') \, \phi(\mathbf{2}, t' + t) \, , \tag{1.20}$$

where T is the time duration of the observation. The cross-correlation is useful as it is a phase-coherent average of inherently random oscillations. It can be seen as a solar seismogram, providing information about travel times, amplitudes, and the shape of the wave packets traveling between any two points on the solar surface. Figure 1.1 shows an example of a surface gravity wave cross-correlation. The positive-time

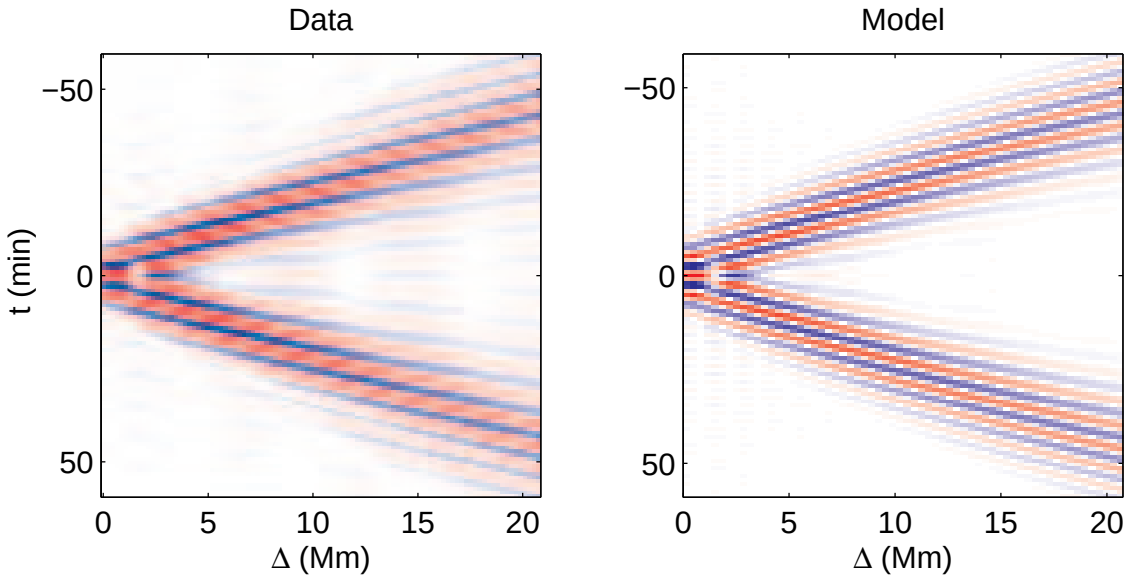

Figure 1.1: Surface gravity wave cross-correlations (Figure 1 from Gizon & Birch, 2002) . The left panel shows an example of an observed cross-correlation $C(\mathbf{1}, \mathbf{2}, t)$ averaged over all possible pairs of points ($\mathbf{1}$,$\mathbf{2}$), as a function of distance $\Delta = \|\mathbf{2} - \mathbf{1}\|$ and time lag t. Red refers to positive values and blue to negative values. The observations are 8-hr time series from the SOHO-MDI high-resolution field of view (Scherrer et al., 1995). The filter $\mathcal{F}$ was chosen to isolate surface gravity waves around 3 mHz. The right panel shows the theoretical cross-correlation from the model which will be discussed in Section 3.4.2.

branch corresponds to waves moving from $\mathbf{1}$ to $\mathbf{2}$, and the negative-time branch represents waves moving in the opposite direction. For acoustic waves there are additional branches, at larger absolute time lag, corresponding to multiple bounces off the surface in between $\mathbf{1}$ and $\mathbf{2}$ (Kosovichev & Duvall, 1997).

Travel Times

The measurement of travel times from cross-correlations is an important part of this dissertation and will be discussed in some detail in section 3.4. As will be discussed later, the ideal definition of travel time is not clear. The intuitive idea is to measure the time lag where the cross-correlation signal is large. This is, in practice, difficult because the cross-correlation is band-limited and therefore spread in time.

Currently, the most accepted approach is to fit a Gaussian wavepacket to the cross-correlation function, obtaining the phase and group times separately (e.g. Chou

& Duvall, 2000). Other approaches include measuring variations in the instantaneous phase (e.g. Chou & Dai, 2001) and fitting a simple model cross-correlation, varying the time shift only (Gizon & Birch, 2002). It is an open question as to which definition is preferable.

1.5.3 Inversions of the Data

In helioseismology the term "inversion" is used to mean the inference of solar structure or flows from observational data. The two most common types of data are travel times and normal mode frequencies. Normal mode frequencies are typically inverted to obtain the north-south and azimuthal average of the sound speed and rotation rate in the solar interior. Travel times have been employed to obtain the meridional flow, rotation rate, supergranular flows, and flows and sound speed around active regions and sunspots. Chapter 4 of this dissertation will demonstrate inversions both of normal mode frequency splittings (m dependence) and travel times.